Supporting Information for Fluoride in the SEI Stabilizes the Li Metal Interface in Li-S Batteries with Solvate Electrolytes

Skyler D. Ware,[†] Charles J. Hansen,[†] John-Paul Jones,[‡] John Hennessy,[‡] Ratnakumar V. Bugga,[‡] and Kimberly A. See[*,†]

†*Division of Chemistry and Chemical Engineering, California Institute of Technology, Pasadena, California 91125, United States*

‡*Jet Propulsion Laboratory, California Institute of Technology, Pasadena, CA 91109, United States*

E-mail: ksee@caltech.edu

Supporting Information

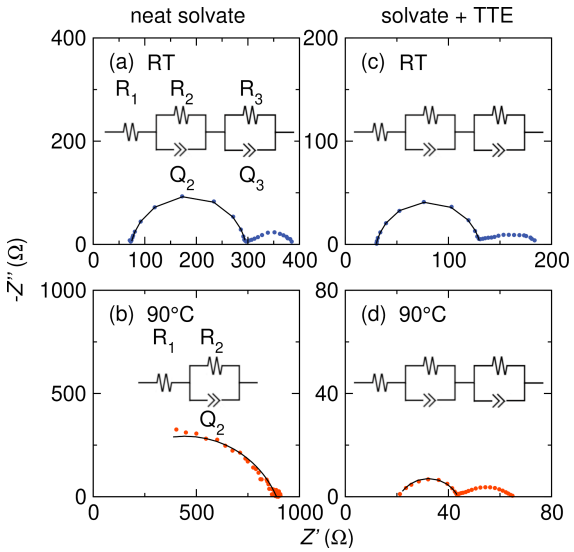

Figure S1: Fits to the high frequency feature of the final collected EIS spectra of Li-Li symmetric cells prepared with (a) neat solvate electrolyte at room temperature, (b) neat solvate electrolyte at 90 °C, (c) solvate + TTE electrolyte at room temperature, and (d) solvate + TTE electrolyte at 90 °C. EIS data was collected from 10^6-10^{-6} Hz (a,c,d) or 10^6-1 Hz (b) at 10 points per decade, with a 10 mV amplitude, continuously for 47 h.

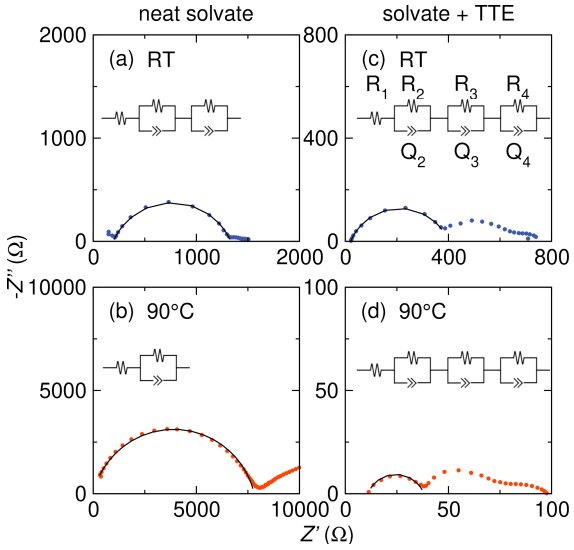

Figure S2: Fits to the high frequency feature of the final collected EIS spectra of AlF_3-coated Li symmetric cells prepared with (a) neat solvate electrolyte at room temperature, (b) neat solvate electrolyte at 90 °C, (c) solvate + TTE electrolyte at room temperature, and (d) solvate + TTE electrolyte at 90 °C. EIS data was collected from 10^6-10^{-6} Hz (a,c,d) or 10^6-1 Hz (b) at 10 points per decade, with a 10 mV amplitude, continuously for 47 h.

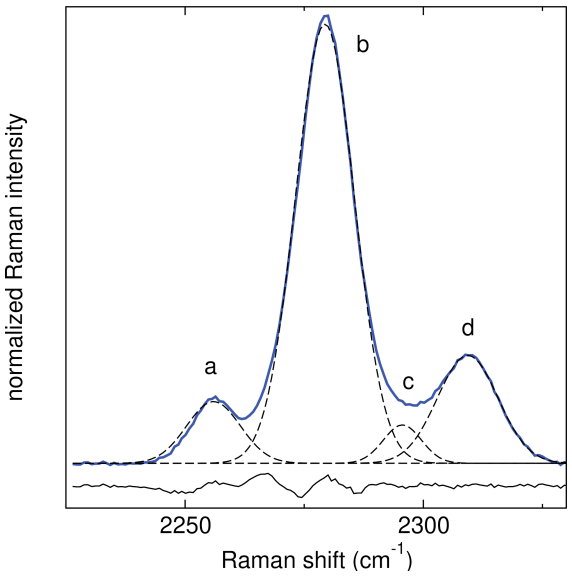

Figure S3: Fits to the room temperature Raman spectrum of MeCN modes in the neat solvate electrolyte.

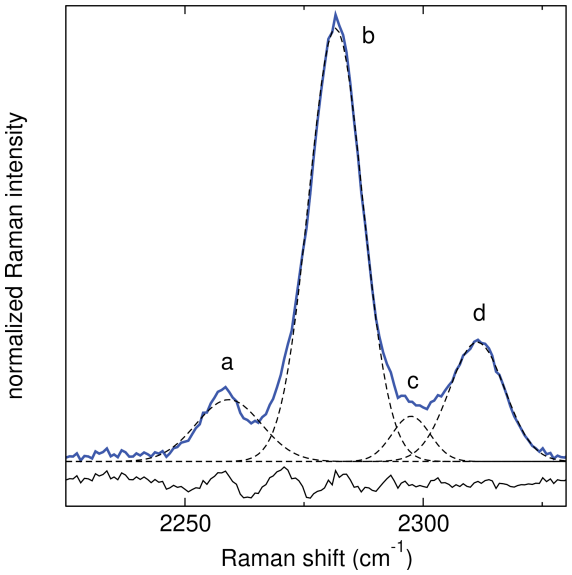

Figure S4: Fits to the room temperature Raman spectrum of MeCN modes in the solvate + TTE electrolyte.

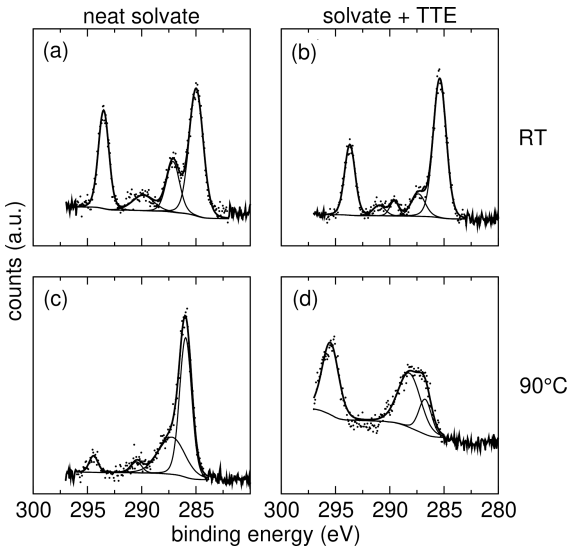

Figure S5: The C 1s spectra of Li metal with reacted with (a) neat solvate electrolyte at RT, (b) solvate + TTE electrolyte at RT, (c) neat solvate electrolyte at 90 °C, and (d) solvate + TTE electrolyte at 90 °C. The lowest binding energy peak in each spectrum was calibrated to 285 eV.

Table S1: Peak assignments of the X-ray photoelectron spectra of Li metal reacted with the neat solvate electrolyte at RT and 90 °C

Figure	**Peak binding energy (eV)**	**Assignment**
4a	532.5	Li_2SO_4
	533.7	Li_2O
4b	400.1	adsorbed MeCN
4c	685.7	LiF
	689.4	TFSI
4d	531.5	Li_2CO_3
	532.5	Li_2SO_4
4e	399.4	CN group
4f	685.7	LiF
	689.4	TFSI

Table S2: Peak assignments of the X-ray photoelectron spectra of Li metal reacted with the solvate + TTE electrolyte at RT and 90 °C

Figure	Peak binding energy (eV)	Assignment
5a	532.2	Li_2SO_4
	533.4	Li_2O
	534.6	impurity
5b	400	adsorbed MeCN
5c	685.4	LiF
	689.1	TTE or TFSI
5d	533.1	SO_4
	531.5	Li_2CO_3
5e	399.9	CN group
5f	685.6	LiF
	686.9	TTE or TFSI
	688.9	TFSI
	690.4	TTE

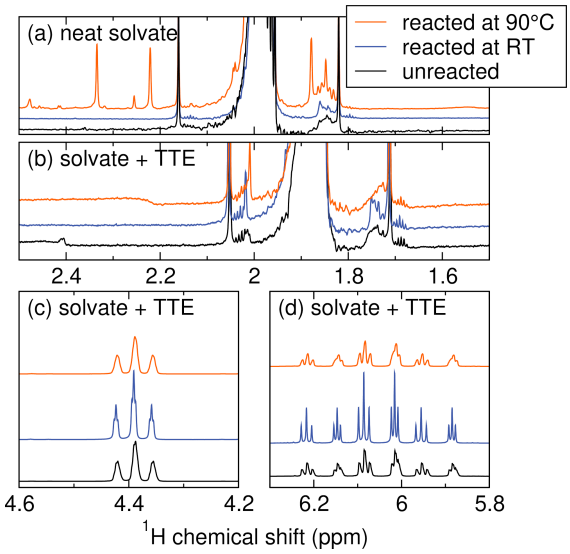

Figure S6: ^{1}H-NMR spectra of (a) the neat solvate electrolyte and (b)-(d) the solvate + TTE electrolyte before and after reaction with Li metal at room temperature and 90 °C. New peaks appear after reaction between the neat solvate electrolyte and Li at 90 °C, indicating electrolyte decomposition. No decomposition is observed after reaction between the solvate + TTE electrolyte at either temperature. The minor shifts in (b) at 1.75 ppm and 2.01 ppm are likely related to negligible changes in coordination structure after heating rather than electrolyte decomposition. The excess deuterated MeCN added as a lock may also affect electrolyte speciation but does not contribute to decomposition.

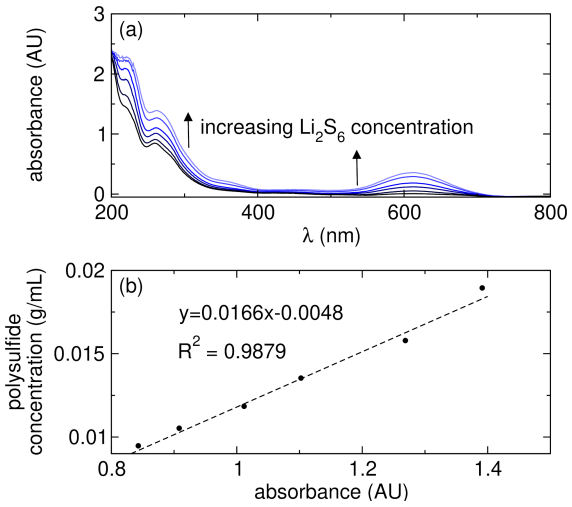

Figure S7: (a) UV-Visible spectra of Li polysulfides in MeCN at RT, with the arrow indicating increasing polysulfide concentration. Peaks corresponding to S_8 (261 nm) and $S_3^{\cdot -}$ (612 nm) are observed due to several disproportionation reactions during polysulfide dissolution. (b) The intensity of the 261 nm peak is plotted against the Li polysulfide concentration in each standard solution to derive a Beer's Law relationship.

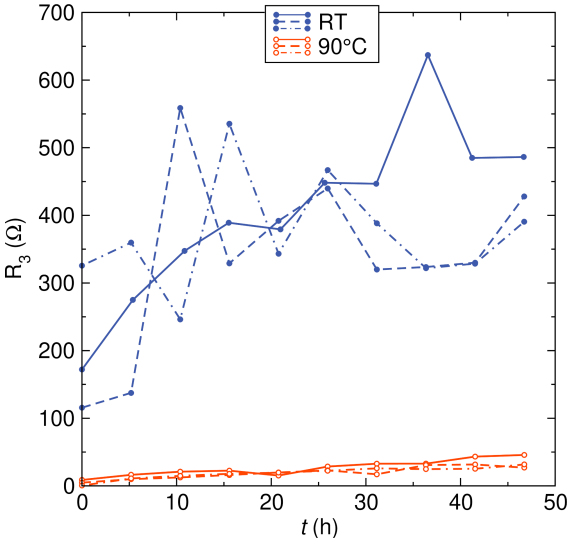

Figure S8: Charge transfer resistance, R_3, from the mid-frequency EIS feature of three replicate AlF_3-coated Li symmetric cells with solvate + TTE electrolyte at room temperature and 90 °C. R_3 increases at both temperatures similarly to R_2. An increase in R_3 may indicate reactivity at the Li/AlF_3 interface.

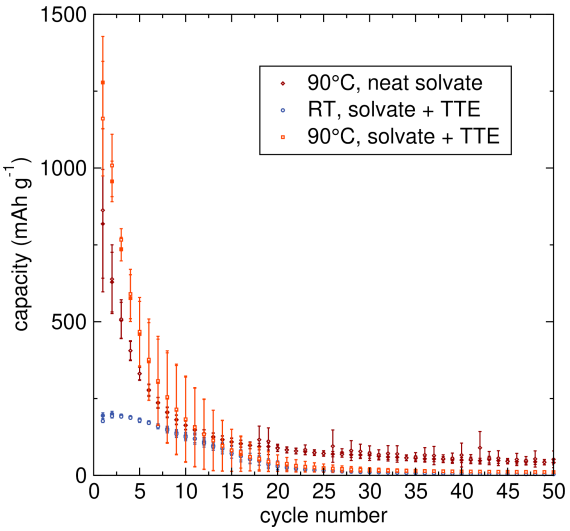

Figure S9: Capacity fade over 50 cycles in AlF_3-coated Li-S cells prepared with both the neat solvate electrolyte and the solvate + TTE electrolyte. Cells cycled at high temperatures yield higher initial capacity but more rapid capacity fade than cells cycled at room temperature. All cells were cycled at C/10 rate.

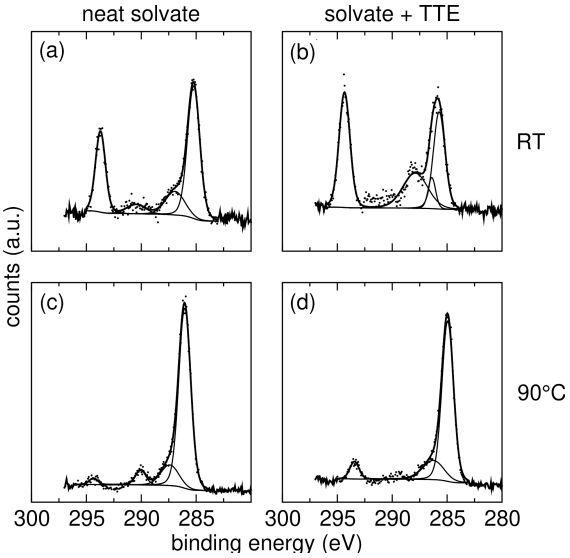

Figure S10: The C 1s spectra of AlF_3-coated Li metal with reacted with (a) neat solvate electrolyte at RT, (b) solvate + TTE electrolyte at RT, (c) neat solvate electrolyte at 90 °C, and (d) solvate + TTE electrolyte at 90 °C. The lowest binding energy peak in each spectrum was calibrated to 285 eV.

Table S3: Peak assignments of the X-ray photoelectron spectra of AlF_3-coated Li metal reacted with the neat solvate electrolyte at RT and 90 °C

Figure	**Peak binding energy (eV)**	**Assignment**
11a	532.3	Li_2SO_4
	533.6	Li_2O
11b	400.1	adsorbed MeCN
11c	689.2	TFSI
	685.4	LiF
11d	531.4	Li_2CO_3
	532.3	Li_2SO_4
	533.6	Li_2O
11e	399.4	CN group
11f	689.2	TFSI
	685.4	LiF

Table S4: Peak assignments of the X-ray photoelectron spectra of AlF_3-coated Li metal reacted with the solvate + TTE electrolyte at RT and 90 °C

Figure	**Peak binding energy (eV)**	**Assignment**
12a	532.5	Li_2SO_4
	533.6	Li_2O
	534.6	impurity
12b	400.1	adsorbed MeCN
12c	689.2	TFSI
	685.4	LiF
	685.9	LiF
12d	532.5	Li_2SO_4
	533.7	Li_2O
12e	400.1	adsorbed MeCN
12f	689.2	TFSI
	685.4	LiF